Physicochemical Interaction Processes in the Carbon (Diamond)−Silicon System

V. Ya. Shevchenko[a], S. N. Perevislov[a, *], and V. L. Ugolkov[a]

[a] Grebenshchikov Institute of Silicate Chemistry, Russian Academy of Sciences, St. Petersburg, 199034 Russia
*e-mail: perevislov@mail.ru

Abstract—The chemical processes occurring during the interaction of carbon (diamond) with silicon are experimentally investigated. Thermal analysis of the interaction of diamond with silicon is carried out. This made it possible to determine the mechanism of the synthesis of silicon carbide and subsequent reaction sintering of diamond particles based on Turing's reaction-diffusion process and the formation of a microstructure consisting of triple periodic surfaces of the minimal energy.

INTRODUCTION

The decisive role in the formation of the properties of substances is played by their chemical nature. However, using composite combinations of various substances, it is possible, in some cases, to obtain the optimal properties of the corresponding materials. Materials based on diamond and heterogeneous silicon carbide are of great practical interest among composites [1, 2].

In order to obtain composites, diamond−silicon carbide uses hot isostatic pressing, spark plasma sintering, and high-pressure sintering. The most effective and practical method is reaction sintering (impregnation of porous billets with Si melt), which leads to the formation of a dense structure consisting of diamond particles and silicon carbide [3–8].

However, despite the significant interest in diamond−silicon carbide composites and the detailed research on their structure, phase composition, and mechanical properties, the physicochemical features of the interaction of diamond with silicon and the formation of a heterodispersed microstructure are still poorly understood.

To create and study materials for the diamond−silicon carbide system, it is necessary to characterize the following basic points:

(1) The microstructure should be a triple periodic structure with the minimal energy, which ensures the possibility of dissipation of the high energies of damage;

(2) H. Shoji et al. [9] showed that as a result of the Turing reaction, a three-dimensional periodicity of the structure can be realized in the material.

(3) The system in which the conditions of the Turing reaction can be created—heterogenetic (the materials are similar in crystal structure but different in properties), for example, diamond and silicon carbide are a heterogenetic pair; i.e., moissanite and diamond coexist in natural formations;

(4) Investigate the possibility of creating conditions for the passage of the Turing reaction in such systems.

(5) Earlier, in purely inorganic systems, there were no such observations.

Some Physicochemical Properties

It is necessary to study in detail the chemistry of the carbon (diamond)−silicon reaction and the formation of silicon carbide as a result of this reaction on the surface of diamond particles, which takes into consideration the crystalline state of SiC, depending on the conditions of the interaction of carbon, graphite, and diamond with silicon.

Silicon carbide has two modifications: hexagonal (α-SiC) and cubic (β-SiC). β-SiC is formed by the interaction of pyrocarbon or a graphite layer of diamond with liquid or gaseous silicon in the course of reactive sintering. The amount of Si in β-SiC can range from 50.0 to 52.5 at %.

The covalent nature and high bond strength C−C in diamond and Si−C in silicon carbide determine their energetic and mechanical strength. In [10], pro-

Table 1. Energy characteristics and properties of diamond, silicon carbide, and silicon

Substance	hkl facets	Ω, kcal/mol	ε, erg/cm^2	σ, erg/cm^2	H, GPa	ΔE, eV
Diamond	100	340	9304	9100	100.0	5.3
β-SiC	100	300	5450	5340	33.4	2.2
Si	100	204	2124	2085	11.0	1.1

Table 2. Parameters of the crystal lattice of diamond, graphite, carbon, silicon carbide, and silicon

Substance	Sphalerite a, Å	Wurtzite		
		a, Å	c, Å	c/a
Diamond	3.5669	—	—	—
Graphite*	—	2.47	6.79	2.749
Carbon**	—	2.52	4.12	1.633
β-SiC	4.3596	—	—	—
α-SiC (2H)	—	3.076	5.048	1.635
Si	5.4306	—	—	—

* Mineral with a layered structure; ** Highly dispersed amorphous carbon.

ceeding from the atomization energy (Ω) of crystals (a function that characterizes the energy strength of a crystal with a covalent lattice), the values of the specific total (ε) and specific free (σ) surface energies were calculated, with which the hardness values (H) and the band gap (ΔE) crystals with a covalent bond are closely correlated (Table 1). Table 2 shows the parameters of the crystal lattice of diamond, graphite, carbon, silicon carbide, and silicon.

Small energy differences between the polytypes allowed the authors of [11] to estimate the probability of the existence of a polytype based on the thermodynamic dependences. The change in the thermodynamic potential during phase transformation is described by the equation:

$$\Delta Z = \Delta H - T\Delta S + P\Delta V. \qquad (1)$$

Since polytypic transitions are not accompanied by noticeable volumetric changes, the term $P\Delta V$ is close to zero. The quantity ΔH is also close to zero, since all SiC polytypes have the same potential energy due to the same environment in the first and second coordination spheres. Thus, the change in free energy (ΔF) for a polytype transition is determined by the difference in the entropy of the initial and final states. Therefore, with a polytypic transition

$$\Delta Z \approx \Delta F \approx -T\Delta S. \qquad (2)$$

Hence it follows that the polytype with a higher level of entropy will be more thermodynamically sustainable.

For the formation of silicon carbide at a temperature of 1800 K, the change in the entropy of synthesis α-SiC (2H) is $\Delta S = 76.79$ J/(mol K); and that of β-SiC, $\Delta S = 76.84$ J/(mol K); therefore, during reac-

tive sintering at a temperature of ~1500°C, the formation of cubic silicon carbide is thermodynamically more probable. At a temperature of 1800°C, the change in the entropy of the α-SiC formation is greater than ΔS of the β-SiC formation, which determines the phase β → α-SiC transition at this temperature.

In the initial period of interaction of diamond particles with silicon, due to the excess of the carbon-containing component (pyrocarbon and graphite on diamond particles), β-SiC of a nonstoichiometric composition (with increased carbon content) is synthesized, which is confirmed by the increase of the lattice parameter to 4.360–4.361 Å [12].

The solubility of carbon in molten silicon largely determines the structure formation of silicon carbide.

The solubility of carbon in solid silicon is very low and even at a temperature of 1410°C does not exceed 0.005 at %. It was shown in [2] that silicon-carbon alloys (up to 0.7% C) are single-phase. Moreover, the lattice parameter in the silicon-based solid solution saturated with carbon noticeably decreases ($a = 5.4174$ Å) compared to pure silicon ($a = 5.4306$ Å) [2]. The increase in the carbon content in the solid solution is also correlated with the microhardness values.

The concentration of carbon in solid silicon (P_C) was calculated based on determining the parameters of the crystal lattice of a solid solution of carbon in silicon, based on the fact that carbon (diamond) and silicon are isomorphic (lattice of the sphalerite type), have a covalent type of chemical bond, and their parameters are linearly related to the carbon concentration. Based on this dependence, the solubility of carbon in silicon can be determined by the formula

$$P_C = \left(\Delta a_p / (2a_{Si} - a_{SiC})\right) \times 100\%, \qquad (3)$$

Table 3. Influence of the type of carbonaceous material and saturation temperature on the solubility of carbon in silicon

Additive to silicon	Saturation temperature, °C	Saturation time, h	Δa_{p}, Å	P_{C}, at %
Carbon	1700	1	−0.0058	0.27
Graphite			−0.0011	0.05
Carbon	2000	0	−0.0065	0.25
Graphite			−0.0066	0.20
Carbon	2200	1	−0.0096	0.45
Graphite			−0.0093	0.43

where Δa_{p} is the absolute value of the change in the lattice parameter of silicon, due to the dissolution of carbon in it; a_{Si} is the silicon lattice parameter; and a_{SiC} is the lattice parameter β-SiC.

In silicon samples saturated with carbon at a temperature of 1250−1350°C, the decrease in the lattice parameter was $\Delta a_{\mathrm{p}} = -0.0020$ Å and $P_{\mathrm{C}} = 0.094$ at %. The solid solution of carbon in silicon in this case is significantly supersaturated, $\Delta a_{\mathrm{p}} = 0.0004 \pm 0.0001$ Å, which corresponds to the carbon concentration $P_{\mathrm{C}} = 0.019$ at %.

As a result of isothermal holding at 1350°C for 18 hours, Δa_{p} becomes equal to −0.0003 Å and does not change with a further increase in the annealing time to 36 h.

Thus, concentration $P_{\mathrm{C}} = 0.019$ at % calculated according to $\Delta a_{\mathrm{p}} = -0.0004$ Å, should be considered the limiting soluble concentration of carbon in silicon at 1250−1350°C, which is maintained upon slow cooling to room temperature.

It was also found that the solubility of carbon in liquid silicon depends not only on the temperature and saturation time but also on the activity of the initial carbon related to the degree of its crystallinity. When micron or submicron, well-crystallized natural graphite (the degree of graphitization is 0.9) dissolves in molten silicon after holding at 1700°C for 1 h and cooling to room temperature, $P_{\mathrm{C}} = 0.052$ at %; and when carbon dissolves (the degree of gravity is 0) under the same conditions, $P_{\mathrm{C}} = 0.27$ at %.

With an increase in the temperature and time of the interaction of carbon and liquid silicon, the difference in the solubilities of carbon and graphite decreases (Table 3).

Graphitization of Diamond Particles

The transformation of diamond into graphite in air begins at a temperature of 800°C [13, 14]. At temperatures below 800°C, the combustion rate exceeds the rate of graphitization. As a result, no graphite layer is formed on the diamond surface. At temperatures above 800°C, the graphitization rate exceeds the combustion rate, and in this case, a thin graphite layer is formed as a result of a surface chemical reaction involving carbon monoxide and carbon dioxide molecules [15]. The thickness of the graphite layer increases with the increasing temperature and pressure of the residual gases [16, 17].

The transition of diamond to graphite in vacuum occurs at a much higher temperature and is explained by the interaction of the surface diamond atoms with oxygen molecules in a vacuum furnace [18]. The thermodynamic analysis shows that the direct transition of diamond to graphite should occur at temperatures above 4000°C [19]. Vacuum graphitization of a perfect diamond crystal is never observed. Graphitization is typical for diamonds which contain microscopic inclusions, especially if they are metallic or graphite.

The authors of [20] consider the complete transition of diamond to graphite rather unlikely. They emphasize the important role of surface chemical reactions and propose a two-stage mechanism, when carbon atoms are first detached from their sites on the diamond surface, forming disordered aggregates, which are then transformed into graphite microcrystals.

In [21], the formation of trigonal pyramids on natural {111} diamond faces upon annealing at a temperature of 1800°C is described. It turned out to be polycrystalline graphite with microcrystals of 10 to 15 nm, predominantly oriented along the {111} diamond face. In [22], the graphitization rate of various diamond faces was investigated; it was found that the {110} face is graphitized faster than the {111} face, although on the surface of the {100} plane there was almost no graphitization. At temperatures above 1600°C, the nature of graphitization changes: it becomes inhomogeneous and anisotropic and penetrates into the crystal. Areas of intense graphitization (graphitization figures) of symmetric shape of up to 100 μm are formed.

In diamond, there are some weak crystallographic planes or directions that are predominantly involved in the graphitization process. On the polished surface of a diamond, the graphitization figures have their shape determined by the symmetry of the diamond lattice. The size and number of such figures increases with the duration and temperature of the sintering of the material. As the process develops, the surface of the diamond is completely covered with a black, uneven layer of graphite.

The investigation of inhomogeneous and anisotropic diamond graphitization in the temperature range 1600−1750°C revealed a different thermal stability of crystal faces; the weakest faces turned out to be in the sequence {211}, {110}, {111}, {100}, {211} [23]. The surface density of atoms on the crystallographic face of diamond {211} is very close to that of atoms on the face of graphite {0001}. In contrast, the {100} faces turned out to be extremely stable against graphitization at material sintering temperatures above 1700°C, and at this temperature all other faces were covered with a continuous layer of graphite.

Graphitization patterns are formed mainly on the roughness of the diamond surface. On polished specimens, they can form on scratches after machining.

The images of graphitization figures recorded at successive sintering stages indicate that they grow from one point. The size of the graphitization figures in the sample plane is 10 times their thickness; i.e., graphitization develops mainly along the surface. For the temperature range 1200−1600°C, the thickness of the graphite layer is determined by the pressure of the residual gases in the vacuum furnace: the better the vacuum the thinner the graphite layer on the diamond surface. And the thinner the layer the higher the temperature at which graphitization figures begin to form.

The factor limiting the propagation of graphitization into the interior of the crystal is pressure, even when graphitization proceeds along planes near the surface of the diamond. Since the density of diamond atoms differs from the density of the resulting graphite layer, the transformation is accompanied by mechanical compression or tension deformations along the plane, which stabilizes the diamond phase. Since the specific volume of graphite is 1.55 times that of diamond, the graphite layers that form below the surface during the diamond-graphite transformation are under pressure from the surface layer of the diamond that they cover. The greater the angles at which the diamond planes {211}, turning into graphite, go deep into the crystal, the more pressure they experience from the side of the covering diamond; this pressure prevents graphitization.

A theoretical model of graphitization was proposed in [24], where the results of the primary principles of molecular dynamics modeling of a surface-induced diamond-graphite transition, which provides a microscopic model for the early stages of the graphitization process, are considered. Penetration of the graphite phase into diamond and vertical graphitization leads to the formation of a coherent diamond−graphite interface.

It can be assumed that the inhomogeneous and anisotropic graphitization of the diamond surface proceeds in several stages:

(1) Formation of a graphitized layer on the diamond surface during heat treatment at temperatures above 800°C due to the interaction of diamond atoms with oxygen molecules and impurities;

(2) Formation of 5−10 nm graphite nuclei on the diamond surface;

(3) Migration of graphite nuclei on the diamond surface and the formation of groups of nuclei with increased density, 10−100 nm in size.

(4) Development of graphitization figures from aggregated cores along the {211} diamond planes, since they have the same surface density as the {0001} graphite planes.

Reactive Sintering Process for Materials Based on Diamond Particles

The reactive sintering process barely affects any of the volume of the diamond particle. The formation of contacts, filling of pores, and the formation of a continuous polycrystalline framework (skeleton) is determined, in this case, by chemical reactions on the diamond surface and is accompanied by the formation of SiC. The synthesis of silicon carbide from elementary silicon and carbon is possible at temperatures significantly lower than the temperature of obtaining liquid-phase sintered and hot-pressed materials. The method of transporting the reacting components during the formation of SiC determines the conditions of the sintering process and the final structure of the material of the diamond-silicon carbide system.

The interaction of solid carbon with silicon melt, the diffusive transfer of dissolved carbon through liquid silicon, the interaction of carbon with gaseous silicon, and the crystallization of SiC from the melt are the main mechanisms that affect the formation of the structure and properties of the material [2].

Let us consider these processes in more detail. The initial porous workpiece is a mixture of diamond particles (D) and pyrocarbon (C) from the pyrolysis of phenol-formaldehyde resin. Such a porous three-phase body (D + C + pores) is impregnated with a silicon melt. Let us imagine the workpiece channels in the form of a cylindrical capillary. Without taking into account the chemical interaction between the melt and the solid phase, the time law of the movement of the meniscus of a liquid in a capillary in a viscous flow has the form [2]:

$$l^2 = \frac{\sigma_{\text{liq,interface}}\cos\theta}{2\eta}R\tau = \frac{\sigma_{\text{liq,interface}}\cos\theta}{2\rho\nu}R\tau \quad (4)$$
$$\text{or } l = k\tau^{1/2},$$

where $k = \frac{\sigma_{\text{liq,interface}}\cos\theta}{2\eta}R = \frac{\sigma_{\text{liq,interface}}\cos\theta}{2\rho\nu}R$, (5)

where η is dynamic viscosity; ν is kinematic viscosity; $\sigma_{\text{liq,interface}}$ is the surface tension of the liquid; ρ is the density of the liquid; θ is the wetting angle; R is the

Table 4. Characteristics of the solubility of carbon and the wettability of diamond particles by silicon

Characteristics	Properties		
Temperature, °C	1420	1500	1600
Wetting angle θ of SiC, deg:			
pure Si	37	32	27
Si saturated with carbon	37	34	31
Wetting angle θ of diamond, deg:			
pure Si	25	22	17
Si saturated with carbon	25	23	20
Solubility of carbon in Si, at %	5.5×10^{-3}	1.3×10^{-2}	4.0×10^{-2}
Silicon density ρ, g/cm^3	2.52	2.49	2.45
Kinetic viscosity ν, cm^2/s	0.00348	0.00265	0.00233

capillary radius; τ is the impregnation time; and l is the impregnation depth.

Equation (4) is valid for describing the kinetics of impregnation of porous materials with melts that do not interact with the solid phase. Table 4 presents data characterizing the effect of the carbon concentration in a silicon melt on the wettability of silicon carbide and diamond.

The impregnation depth l of a porous body made of diamond and silicon carbide particles can be calculated. The surface tension of silicon in the temperature range 1420−1600°C barely changes and is equal to 860 dyn/cm [2]. The dependence of the impregnation depth l of porous blanks based on silicon carbide and diamond particles versus time τ is shown in Fig. 1 in the temperature range 1420−1600°C, subject to the pore radius $R = 10$ μm.

It can be seen from the analysis of the graphs that at a temperature of 1420°C, good impregnation of the porous workpieces based on silicon carbide and diamond particles is noticeable. Workpieces made of diamond particles are impregnated with liquid silicon better because the wetting angle θ of diamond particles with silicon is lower than when wetting SiC; this is probably due to the partial graphitization of diamond (the wetting angle of graphite with silicon is 0°).

With increasing temperature, the region between the lines of impregnation of silicon carbide and diamond narrows, since the wetting angle of silicon carbide and diamond with silicon decreases. The rate of impregnation also depends on the effective pore radius (in our calculation $R = 10$ μm). Upon the contact of porous blanks with liquid silicon, immediately after its melting, the impregnation proceeds relatively quickly
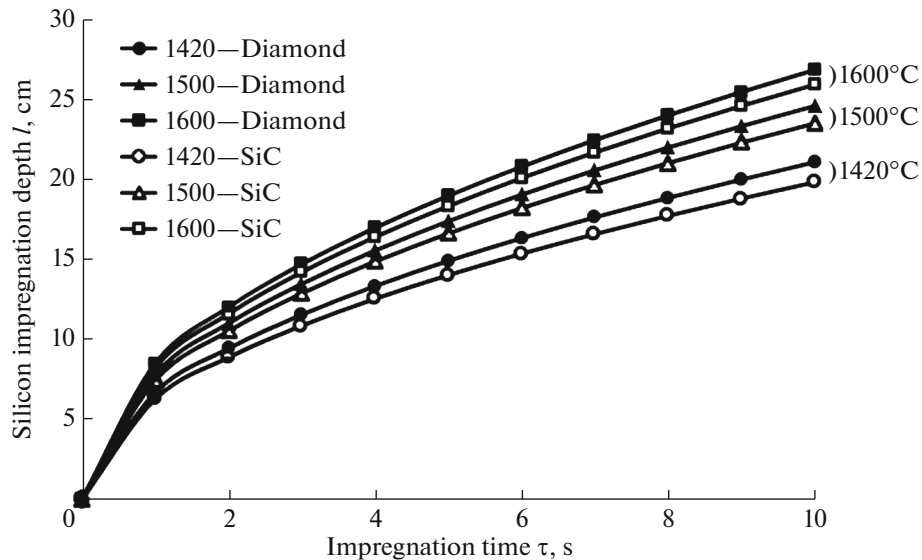

Fig. 1. Dependence of the depth of impregnation of porous workpieces based on silicon carbide and diamond particles on the time of impregnation.

to a sufficiently large depth. Therefore, even for large items of 25 to 30 cm, the impregnation time is about 10 s.

The system we are considering includes chemical interactions between the carbon and silicon melt. Therefore, in order to analyze the phenomena occurring during the impregnation of a two-component porous workpiece, the following two particular systems should be considered separately: $C–Si_{liq}$ and $D–Si_{liq}$.

The impregnation of porous carbon (graphite) with chemically active melts is considered in [25, 26]. In [27, 28], the kinetics of impregnation of porous graphites with liquid silicon was experimentally studied. It was found that at the initial stage of the process (0–50 s), the impregnation depth l obeys the equation $l = k'\tau^{1/2}$, which is typical for a viscous fluid flow.

It was shown in [25] that in cases where complete wetting is observed and the driving force of the impregnation process remains practically constant with the change in temperature, the activation energy of impregnation becomes comparable to the activation energy of the viscous flow of the impregnating liquid.

The viscous nature of the flow of a silicon melt during impregnation of graphite is also confirmed by the value of the activation energy, determined in the temperature range 1410–1550°C. The activation energy of impregnation of graphite with silicon fluctuates at the initial stage of the process in the range 11.5–14.2 kcal/mol for different grades of graphite, which is in good agreement with the activation energy of the viscous flow of silicon, which is 10.3–10.6 kcal/mol for these temperatures [27, 28].

With increasing time (50–180 s), the depth of impregnation becomes proportional to $\tau^{1/4}$, which is related to the surface diffusion of silicon. In this case, the activation energy of the process increases to 45–53 kcal/mol.

The results obtained indicate that at the initial stage, the process of impregnation of carbon (graphite) with silicon is determined by a viscous flow and is not complicated by the formation of silicon carbide, which begins to crystallize at the interface after saturation of the melt with carbon.

Thus, the following elementary processes are assumed during the reactive sintering of materials based on diamond particles: wetting and impregnation of a solid porous body with molten silicon; and dissolution of pyrocarbon and graphite on the surface of diamond particles in a silicon melt. Silicon carbide is synthesized as a result of the heterogeneous interaction ($Si_{liq} + C_{sol} = SiC_{sol}$) and the transfer of carbon through the silicon melt with the subsequent crystallization of SiC on the surface of diamond particles as a result of the reactive-diffusive interaction, i.e., Turing's reaction.

Sintering of Diamond and Solid Carbon Particles in the Presence of Molten Si

In order to consider the mechanism of the reactive sintering of materials based on diamond particles, we present a model consisting of an ensemble of spherical particles. For example, four diamond particles, the carbon particles between them, and a space filled with molten silicon (Fig. 2a). This model is implemented at the initial stage of the process as a result of the impregnation of porous workpieces consisting of particles of diamond, carbon, and molten Si (Fig. 2a).

The next stage is the dissolution of carbon (pyrocarbon) and graphite on the surface of the diamond, saturation of the silicon melt with them, and crystallization in the form of silicon carbide in the most favorable places in thermodynamic terms, i.e., on the surfaces of diamond particles (Fig. 2b). Moreover, this process does not lead to a change in the center distances of the contacting spheres of diamond particles. The dissolving carbon atoms diffuse at the melt–carbon and melt–diamond boundaries and directly crystallize from the melt in the form of silicon carbide grains. Therefore, it can be expected that the concentration of carbon in silicon will not reach the equilibrium value until the moment of the complete dissolution of the carbon (graphite) particles.

The formation of silicon carbide on diamond particles and on SiC particles during the reactive sintering of silicon carbide occurs in accordance with the reaction-diffusion Turing mechanism layer-by-layer (Fig. 2), thus forming triple periodic surfaces (Turing fences) in the volume of the diamond frame.

Thus, as long as a liquid silicon phase exists in the material in contact with solid carbon, an intense transfer of carbon through the melt and deposition of SiC in the form of grains on the surface of the diamond particles will occur (Fig. 2c).

The self-diffusion coefficient of silicon and the diffusion coefficient of carbon in liquid silicon are as follows:

$$D_C \approx D_{Si} = 0.755 \times 10^{-3} \exp\left(-\frac{9150}{RT}\right). \quad (6)$$

Calculations using this formula give the following values for the diffusion coefficient:

Temperature, °C	Diffusion coefficient $D \times 10^5$, cm²/s
1420	5.19
1500	5.55
1600	6.38
2000	9.87

The diffusion coefficient of carbon through liquid silicon is 6–7 orders of magnitude higher than the diffusion coefficient of carbon through the silicon carbide layer and 9–10 orders of magnitude higher than

the diffusion coefficient of carbon through the diamond layer.

Based on these diffusion coefficients, in our study, we calculated the time of the complete transformation of silicon upon interaction with carbon (graphite) into silicon carbide during reactive sintering, which at 1700°C is 2.58×10^4 s (~7 h); and at 2100°C, ~18 min.

Reaction-Diffusion Turing Mechanism

The Si−C phase diagram (Fig. 3) shows that in a region rich in carbon (more than 50 at % C) there are only two phases SiC and C, and Si completely transforms into silicon carbide [29]. At the initial stage of impregnation, liquid Si penetrates into the pore channels of the workpiece and interacts with carbon, the amount of which exceeds Si, to form silicon carbide. The further reaction of interaction of silicon with carbon is carried out by the diffusion of Si through the SiC layer. Therefore, the reaction process involves the diffusion of silicon atoms through the silicon carbide layer and the reaction between Si and carbon. The kinetics of the reaction is very slow because of the low diffusion coefficients of C and Si in SiC [30], which leads to the formation of SiC layers on the surface of the diamond particles.

The process of SiC formation can be explained from the point of view of the analysis of the reaction-diffusion mechanism by A. Turing [31]. The source of carbon in materials based only on diamond particles is graphite, which at high temperatures can partially graphitize on the surface (the diamond-graphite phase transition occurs). The analysis of the kinetics of the growth of the SiC layer as a result of the reactive-diffusive interaction between diamond and silicon [32], confirmed experimentally, showed the formation of an SiC layer on the surface of diamond particles.

Accordingly, proceeding from the Turing reaction-diffusion mechanism, nanosized grains of SiC are formed on the surface of diamond particles with the diffusion of gaseous Si into a porous workpiece, and when impregnated with a liquid silicon melt of pyrocarbon and graphite particles on the diamond surface, micron grains of SiC are formed, forming in both cases a Turing fence (Fig. 4).

The pressure of saturated gaseous Si is 1 Pa at a temperature of 1500°C [33]; therefore, Si penetrates into the porous workpiece at a high speed and, on coming into contact with carbon, forms silicon carbide. As shown earlier, saturation with liquid silicon occurs due to the capillary impregnation of the porous workpiece.

The reaction-diffusion interaction of Si with carbon is accompanied by an exothermic effect (an increase in the temperature of the system to 2400°C), with the enthalpy $H_0 = -117.77$ kJ/mol, which eliminates temperature gradients in the workpieces [34]. As a result, the rate of dissolution of pyrocarbon and graphite on diamond particles in liquid Si increases.
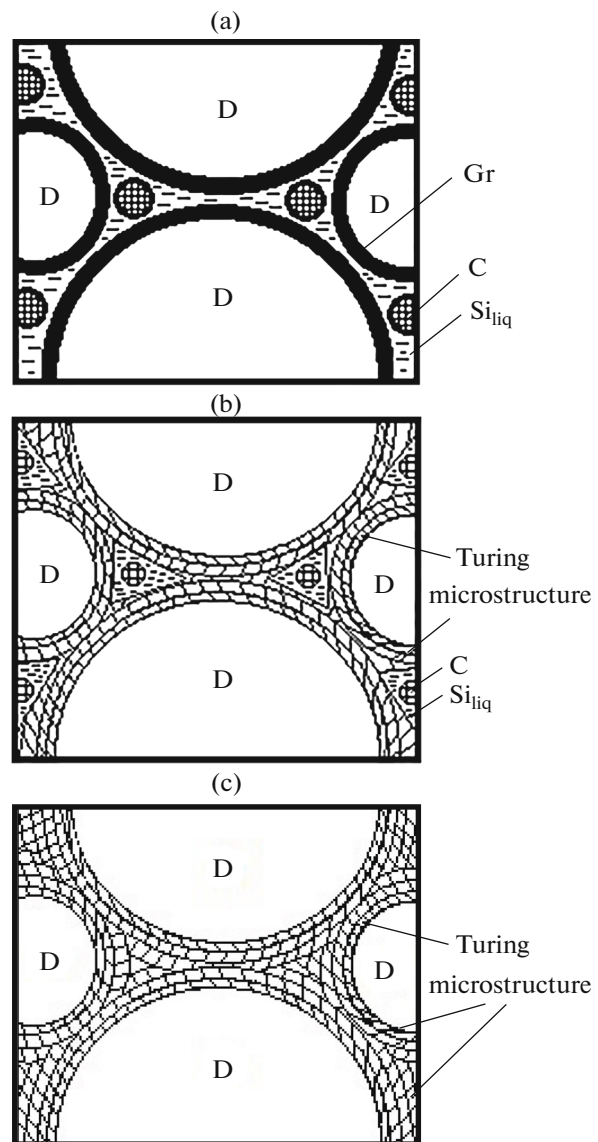

Fig. 2. Model scheme for the distribution of phase components at stage I (a), Stage II (b) and stage III (c) reaction sintering. The diagram shows the following phases: Diamond (D); graphite on the surface of diamond particles (Gr); pyrocarbon (C); liquid silicon (Si$_{liq}$); silicon carbide (SiC) and SiC formed as a result of reaction-diffusion interaction on the surface of diamond particles (Turing fence).

The viscosity of Si and the wetting angle of carbon with it decrease, which leads to faster and easier impregnation of the porous workpiece with liquid Si. The diffusion rate of Si increases by several hundred percent, and the pores of the diamond material blank are filled with SiC, in accordance with the Turing reaction-diffusion mechanism.

Thermal Analysis of the Diamond-Silicon System

For the experimental study of the processes of interaction of diamond with silicon, a complex thermal analysis was carried out. The TG and DSC studies
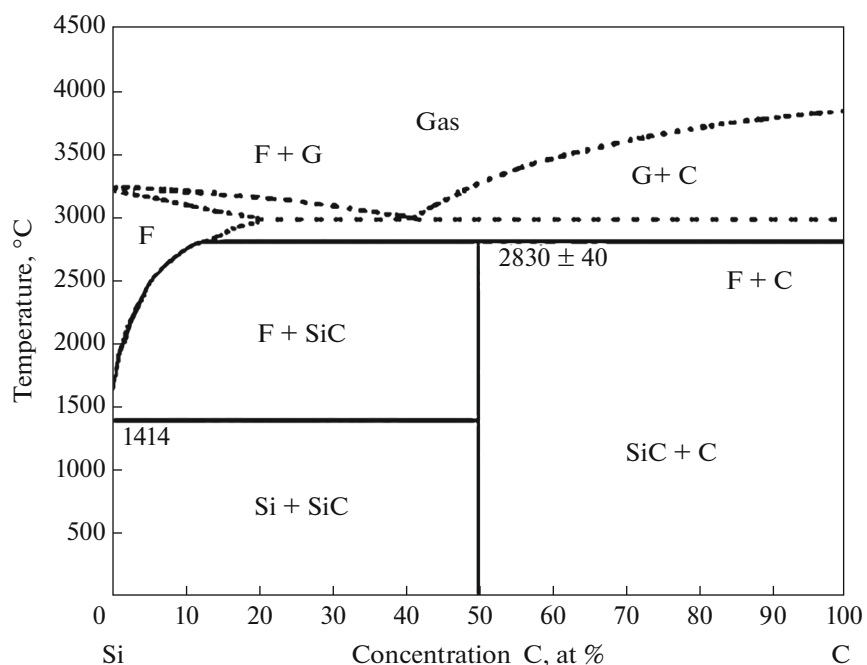
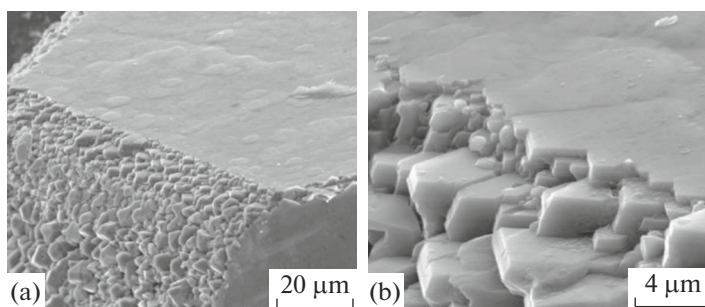**Fig. 3.** Diagram of phase equilibria of the Si–C system.

Fig. 4. Formation of micron grains SiC (Turing's fence) formed during the interaction of a graphite layer on the surface of a diamond particle with liquid Si (a, b).

were carried out on an STA 429 CD complex thermal analysis unit produced by NETZSCH (Germany).

Sample 1, consisting of diamond powder of a fraction of 20/28 mm, in the form of a disk of ⌀5 mm, $h = 1$ mm, and a porosity of 45 vol %, was placed in an open alundum crucible. A particle of monocrystalline silicon was placed on the upper surface of the disk (Fig. 5a).

The sample was subjected to complex thermal analysis when heated at a rate of 20°C/min in a dynamic Ar atmosphere (Ar flow of 50 cm³/min) in the temperature range 40–1500°C and cooling up to 1200°C. Ar was pumped in after evacuating the furnace air to 1×10^{-4} mbar. The decomposition products were analyzed using a QMS 403 C quadrupole mass spectrometer (NETZSCH, Germany) connected to an oven.

The aim of the research was to study the features of the processes occurring during the heat treatment of diamond–silicon composites and to experimentally confirm the interaction of the components with the formation of silicon carbide.

Figure 6 shows the TG and DSC curves of sample 1 heat treated in the temperature range 40–1500°C at a speed of 20°C/min in a stream of Ar.

The TG curve shows that the mass of the sample decreases throughout the heating period from 100 to 1500°C. The weight loss of the sample at a temperature of 1500°C is 0.79% (Fig. 6), which indicates the absence of interaction with the formation of gaseous products. When the sample is cooled in the temperature range 1500–1200°C, there is practically no change in mass.
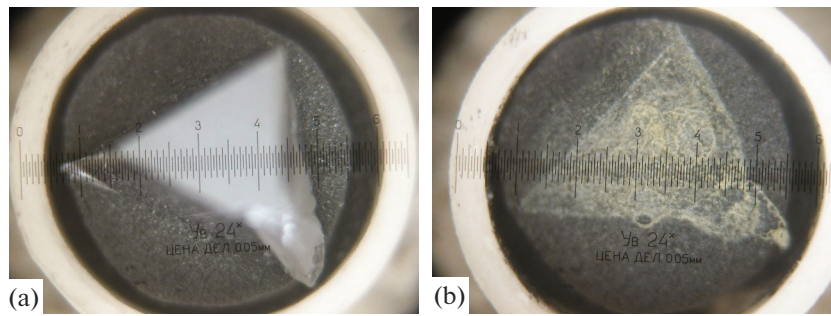
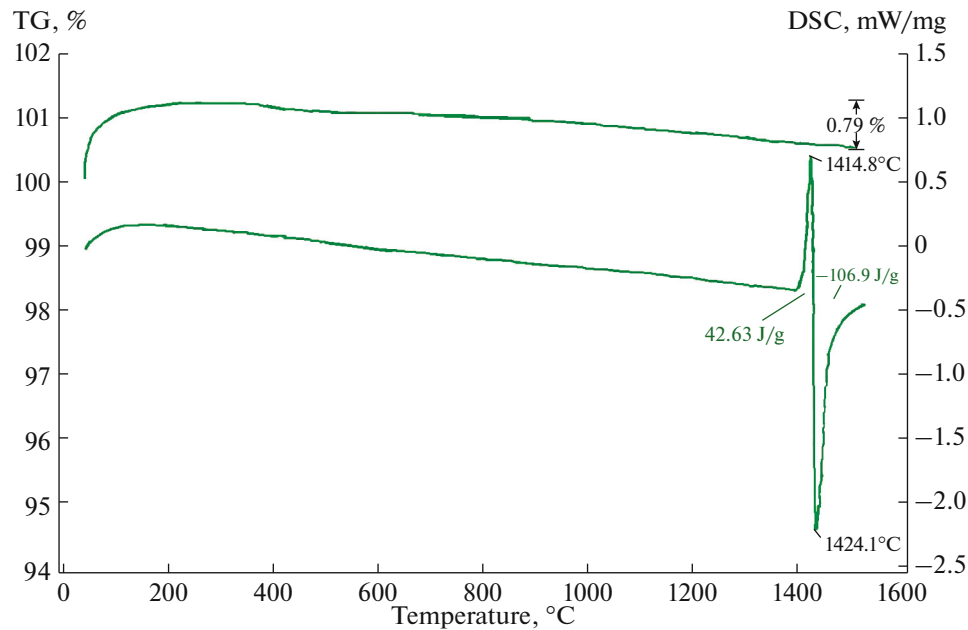**Fig. 5.** Micrographs of sample *1* up to (a) and after (b) heat treatment. Magnification 24×.

Fig. 6. TG and DSC curves obtained during heat treatment of sample *1* in the temperature range 20−1500°C.

The DSC curve when heated (Fig. 6) to a temperature of 1390.8°C (the heat of fusion is −0.3469 mW/mg) is smooth. At a temperature of 1390.8°C, the process of silicon melting begins, accompanied by a large endothermic effect (the specific heat of the chemical reaction is 42.63 J/g). The maximum of the peak is observed at a temperature of 1414.8°C (the heat of fusion is 0.6937 mW/mg), which corresponds to the complete melting of silicon and its penetration into the porous diamond sample. The dissolution of graphite (carbon) on the surface of the diamond particles and the formation of silicon carbide begin at this temperature, accompanied by a large exothermic effect (the specific heat of the chemical reaction is −106.9 J/g). The DSC curve moves sharply downward to the minimum at 1424.1°C (the heat of crystallization is −2.196 mW/mg). The exothermic effect ends at a temperature of 1444.7°C (the heat of crystallization is −0.4988 mW/mg).

It should be noted that the time between the maximum melting point of silicon (1414.8°C) and the maximum crystallization temperature of silicon carbide (1424.1°C) is about 28 s. This confirms the correctness of the calculation of the impregnation time of the porous diamond workpiece (Fig. 1).

Figure 7 shows the DSC curves of sample 1 (solid line) and sample 2 (dashed line), annealed in the temperature range 1300−1500°C at a speed of 20°C/min in a stream of Ar (50 mL/min). Sample 2 consisted of diamond powder of a 20/28 mm fraction, in the form of disks of ∅5 mm and $h = 1$ mm, which was pretreated at a temperature of 1300°C in the Ar environment. After that, a single-crystal silicon particle was placed on the upper surface of the disk, similarly to sample 1 (Fig. 5a).

Since samples 1 and 2 practically did not differ in the mass, nature, and fractional composition of diamond, except for the preliminary heat treatment of
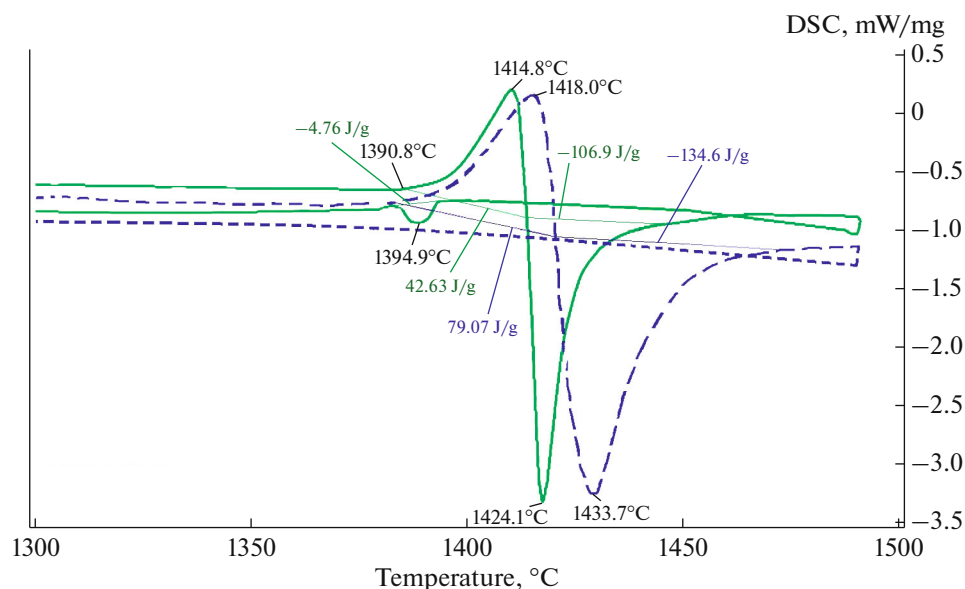
Fig. 7. DSC curves obtained during heat treatment of sample 1 (solid line) and sample 2 (dashed line) in the temperature range 1300−1500°C.

sample 2 at 1300°C, and it is interesting to compare their reactivity and behavior during the heat treatment.

The DSC curve of sample 1 (Fig. 7) repeats the results shown in Fig. 6. The formation of liquid silicon and silicon carbide for sample 1 begins a little earlier (1414.8 and 1424.1°C) than for sample 2 (1418.0 and 1433.7°C); and the difference in the temperatures of the onset of the silicon carbide formation process was 9.6°C. The heat release for sample 1 stopped at 1444.7°C; and for sample 2, at a temperature of 1472.2°C. Thus, the preliminary heat treatment of diamond powder (sample 2) leads to a slight retardation of the SiC formation process.

If we compare the specific heat values of the chemical reactions of silicon melting and silicon carbide crystallization—42.63 and −106.9 J/g for sample 1, and 79.07 and −134.6 J/g for sample 2—in the latter, during the crystallization of SiC, a large amount of energy is released, which is related to the formation of a larger amount of silicon carbide.

During the cooling of sample 1, an exothermic effect was observed (the specific heat of the chemical reaction was −4.76 J/g) of the crystallization of liquid silicon, which did not react with graphite, starting at a temperature of 1394.9°C (the heat of crystallization was −0.4792 mW/mg). The temperature of the onset of silicon crystallization (1394.9°C) practically coincides with the beginning of its melting (1390.8°C).

When sample 2 was cooled, no exothermic peak was observed, which also indicates the formation of a larger layer of graphite on the diamond particles of sample 2 (preheat treated at 1300°C), which is most likely sufficient for the complete reaction between graphite and silicon to form silicon carbide. Therefore,

no exothermic effect is observed on the DSC curve of sample 2 during cooling (Fig. 7).

Figure 5 shows micrographs of a sample (tablets with silicon) before heat treatment at 1490°C (Fig. 5a) and after heat treatment (Fig. 5b). After heat treatment, a silicon crystal contour remains on the upper surface of the sample. It is possible that a thin silicon film remains in the place where the crystal is absorbed into the porous workpiece.

Microstructure Analysis

Figure 8 shows the microstructure of a diamond-silicon carbide composite. The dark phases correspond to diamond particles; and the light gray phases,
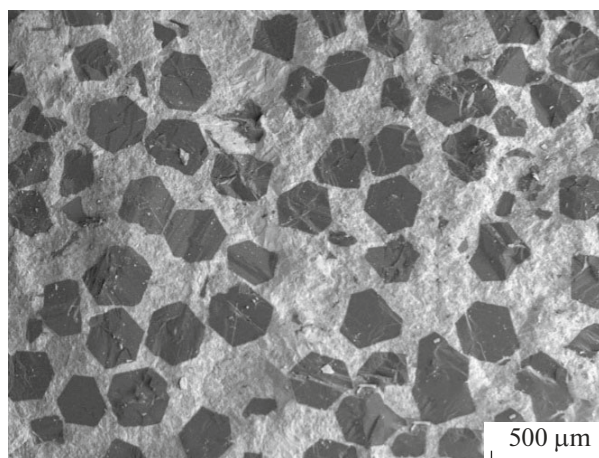

Fig. 8. Microstructure of reactive-sintered diamond-silicon carbide material.

to β-SiC. Diamond crystals with a regular shape are uniformly distributed in the composite. There are practically no pores in the material, which indicates a strong interfacial bond between diamond and silicon carbide.

CONCLUSIONS

Physicochemical interactions in the carbon (diamond)−silicon system have been investigated. The nature of the process of the reactive sintering of carbon (diamond) with silicon is studied; models of sintering particles of diamond, carbon, and diamond with carbon in the presence of molten silicon are considered; and thermal analysis is conducted of the interaction of diamond with silicon, which helped explain the interaction of diamond particles with silicon based on the model of the reaction-diffusion Turing mechanism and material production with a microstructure consisting of triple periodic surfaces of the minimal energy.

FUNDING

CONFLICT OF INTEREST

The authors declare that they have no conflict of interest.

OPEN ACCESS

REFERENCES

1. Shevchenko, V.Ya., Glass and ceramics, in *XXI. Perspektivy razvitiya* (XXI. Development Prospects), St. Petersburg: Yanus, 2001.

2. Knippenberg, W.F., Growth phenomena in silicon carbide, *Philips Res. Rep.,* 1963, vol. 18, pp. 161−274.

3. Ekstrom, T.C. and Gordeev, S.K., New carbide composites with extraordinary properties, *Key Eng. Mater.,* 1999, pp. 75−80.

4. Park, J.S., Sinclair, R., Rowcliffe, D., Stern, M., and Davidson, H., Orientation relationship in diamond and silicon carbide composites, *Diamond Relat. Mater.,* 2007, vol. 16, no. 3, pp. 562−565.

5. Liu, Y., Hu, C., Feng, W., Men, J., Cheng, L., and Zhang, L., Microstructure and properties of diamond/SiC composites prepared by tape-casting and chemical vapor infiltration process, *J. Eur. Ceram. Soc.,* 2014, vol. 34, no. 15, pp. 3489−3498.

6. Matthey, B., Kunze, S., Hörner, M., Blug, B., van Geldern, M., Michaelis, A., and Herrmann, M., SiC-bonded diamond materials produced by pressureless silicon infiltration, *J. Mater. Res.,* 2017, vol. 32, no. 17, pp. 3362−3371.

7. Taylor, A., Klimša, L., Kopeček, J., Remeš, Z., Vronka, M., Čtvrtlík, R., Tomáštík, J., and Mortet, V., Synthesis and properties of diamond-silicon carbide composite layers, *J. Alloys Compd.,* 2019, vol. 800, pp. 327−333.

8. Salamone, S., Aghajanian, M., Horner, S.E., and Zheng, J.Q., Reaction bonded SiC/diamond composites: Properties and impact behavior in high strain rate applications, *Adv. Ceram. Armor XI,* 2015, vol. 600, pp. 111−118.

9. Shoji, H. and Ohta, T., Computer simulations of three-dimensional turing patterns in the Lengyel−Epstein model, *Phys. Rev. E,* 2015, vol. 91, no. 3, p. 032913.

10. Müller, U., *Inorganic Structural Chemistry,* New York: Wiley, 2006.

11. Belenkov, E.A., Agalyamova, E.N., and Greshnyakov, V.A., Classification and structure of silicon carbide phases, *Phys. Solid State,* 2012, vol. 54, no. 2, pp. 433−440.

12. Falk, A.L., Buckley, B.B., Calusine, G., Koehl, W.F., Dobrovitski, V.V., et al., Polytype control of spin qubits in silicon carbide, *Nat. Commun.,* 2013, vol. 4, no. 1, pp. 1−7.

13. Howes, V.R., The graphitization of diamond, *Proc. Phys. Soc.,* 1962, vol. 80, no. 3, p. 648.

14. Harris, J.W. and Vance, E.R., Induced graphitisation around crystalline inclusions in diamond, *Contrib. Mineral. Petrol.,* 1972, vol. 35, no. 3, pp. 227−234.

15. Evans, T. and Sauter, D.H., Etching of diamond surfaces with gases, *Philos. Mag.,* 1961, vol. 6, no. 63, pp. 429−440.

16. Dallek, S., Kabacoff, L., and Norr, M., Oxidation kinetics of type 2A natural diamond [100] and [111] surfaces by TG, *Thermochim. Acta,* 1991, vol. 192, pp. 321−326.

17. Sun, Q. and Alam, M., Relative oxidation behavior of chemical vapor deposited and type II a natural diamonds, *J. Electrochem. Soc.,* 1992, vol. 139, no. 3, pp. 933−936.

18. Van Enckevort, W.J.P. and de Theije, F.K., Etching of diamond, in *Properties, Growth and Application of Diamond,* Nazare, M.H. and Neves, A.J., Eds., London: Inst. Electr. Eng., 2001, pp. 115−124.

19. Bundy, F.P., Bassett, W.A., Weathers, M.S., Hemley, R.J., Mao, H.U., and Goncharov, A.F., The pressure-temperature phase and transformation diagram for carbon; Updated through 1994, *Carbon,* 1996, vol. 34, no. 2, pp. 141−153.

20. Davies, G. and Evans, T., Graphitization of diamond at zero pressure and at a high pressure, *Proc. R. Soc. London, Ser. A,* 1972, vol. 328, no. 1574, pp. 413−427.

21. Xie, H., Yin, F., and Yu, T., Strain rate induced graphitization of cubic diamond film, *Appl. Phys. Lett.,* 2014, vol. 104, no. 3, p. 031911.

22. Butenko, Yu.V., Kuznetsov, V.L., Chuvilin, A.L., Kolomiichuk, V.N., Stankus, S.V., Khairulin, R.A., and Segall, B., Kinetics of graphitization of dispersed diamonds at low temperatures, *Zh. Prikl. Fiz.,* 2000, vol. 88, no. 7, pp. 4380−4388.

23. Khmelnitsky, R.A. and Gippius, A.A., Transformation of diamond to graphite under heat treatment at low pressure, *Phase Trans.,* 2014, vol. 87, no. 2, pp. 175−192.

24. De Vita, A., Galli, G., Canning, A., and Car, R., A microscopic model for surface-induced diamond-to-graphite transitions, *Nature* (London, U.K.), 1996, vol. 379, no. 6565, pp. 523−526.

25. Canham, L.T., Houlton, M.R., Leong, W.Y., Pickering, C., and Keen, J.M., Atmospheric impregnation of porous silicon at room temperature, *J. Appl. Phys.,* 1991, vol. 70, no. 1, pp. 422−431.

26. Lee, J., Kim, J., and Hyeon, T., Recent progress in the synthesis of porous carbon materials, *Adv. Mater.,* 2006, vol. 18, no. 16, pp. 2073−2094.

27. Sibieude, F. and Benezech, G., Chemical vapour deposition of silicon carbide: An X-ray diffraction study, *J. Mater. Sci.,* 1988, vol. 23, no. 5, pp. 1632−1636.

28. Fleisher, A., Zolotaryov, D., Kovalevsky, A., Muller-Kamskii, G., Eshed, E., Kazakin, M., and Popov, V.V., Jr., Reaction bonding of silicon carbides by binder jet 3D-printing, phenolic resin binder impregnation and capillary liquid silicon infiltration, *Ceram. Int.,* 2019, vol. 45, no. 14, pp. 18023−18029.

29. Ohtaka, O., Shimono, M., Ohnishi, N., Fukui, H., Takebe, H., Arima, H., and Kume, Sh., HIP production of a diamond/SiC composite and application to high-pressure anvils, *Phys. Earth Planet. Inter.,* 2004, vol. 143, pp. 587−591.

30. Zollfrank, C. and Sieber, H., Microstructure evolution and reaction mechanism of biomorphous SiSiC ceramics, *J. Am. Ceram. Soc.,* 2005, vol. 88, no. 1, pp. 51−58.

31. Turing, A., The chemical basis of morphogenesis, *Phil. Trans. R. Soc. London, Ser. B,* 1952, vol. 237, no. 641, pp. 37−72.

32. Mlungwane, K., Sigalas, I., Herrmann, M., and Rodriguez, M., The wetting behaviour and reaction kinetics in diamond−silicon carbide systems, *Ceram. Int.,* 2009, vol. 35, no. 6, pp. 2435−2441.

33. Haynes, W.M., *CRC Handbook of Chemistry and Physics*, Boca Raton: CRC, 2014.

34. Shevchenko, V.Y., Koval'chuk, M.V., and Oryshchenko, A.S., Synthesis of a new class of materials with a regular (periodic) interconnected microstructure, *Glass Phys. Chem.,* 2019, vol. 45, no. 6, pp. 412−418.